Balancing Power Absorption and Structural Loading for an Assymmetric Heave Wave-Energy Converter in Regular Waves

Preprint

Nathan M. Tom
National Renewable Energy Laboratory

Farshad Madhi and Ronald W. Yeung
University of California at Berkeley

Presented at the ASME 2016 35th International Conference on Ocean, Offshore and Arctic Engineering (OMAE2016)
Busan, South Korea
June 19–24, 2016

NREL is a national laboratory of the U.S. Department of Energy
Office of Energy Efficiency & Renewable Energy
Operated by the Alliance for Sustainable Energy, LLC

This report is available at no cost from the National Renewable Energy Laboratory (NREL) at www.nrel.gov/publications.

Conference Paper
NREL/CP-5000-65656
July 2016

Contract No. DE-AC36-08GO28308

NOTICE

This report is available at no cost from the National Renewable Energy Laboratory (NREL) at www.nrel.gov/publications.

Available electronically at SciTech Connect http:/www.osti.gov/scitech

Available for a processing fee to U.S. Department of Energy and its contractors, in paper, from:

U.S. Department of Energy
Office of Scientific and Technical Information
P.O. Box 62
Oak Ridge, TN 37831-0062
OSTI http://www.osti.gov
Phone: 865.576.8401
Fax: 865.576.5728
Email: reports@osti.gov

Available for sale to the public, in paper, from:

U.S. Department of Commerce
National Technical Information Service
5301 Shawnee Road
Alexandra, VA 22312
NTIS http://www.ntis.gov
Phone: 800.553.6847 or 703.605.6000
Fax: 703.605.6900
Email: orders@ntis.gov

Cover Photos by Dennis Schroeder: (left to right) NREL 26173, NREL 18302, NREL 19758, NREL 29642, NREL 19795.

NREL prints on paper that contains recycled content.

BALANCING POWER ABSORPTION AND STRUCTURAL LOADING FOR AN ASYMMETRIC HEAVE WAVE-ENERGY CONVERTER IN REGULAR WAVES

Nathan M. Tom[*]
National Renewable Energy Laboratory
National Wind Technology Center
Golden, Colorado, 80401
Email: nathan.tom@nrel.gov

Farshad Madhi[†]
University of California at Berkeley
Department of Mechanical Engineering
Berkeley, California, 94720
Email: madhi@berkeley.edu

Ronald W. Yeung[‡]
University of California at Berkeley
Department of Mechanical Engineering
Berkeley, California, 94720
Email: rwyeung@berkeley.edu

ABSTRACT

The aim of this paper is to maximize the power-to-load ratio of the Berkeley Wedge: a one-degree-of-freedom, asymmetrical, energy-capturing, floating breakwater of high performance that is relatively free of viscosity effects. Linear hydrodynamic theory was used to calculate bounds on the expected time-averaged power (TAP) and corresponding surge restraining force, pitch restraining torque, and power take-off (PTO) control force when assuming that the heave motion of the wave energy converter remains sinusoidal. This particular device was documented to be an almost-perfect absorber if one-degree-of-freedom motion is maintained. The success of such or similar future wave energy converter technologies would require the development of control strategies that can adapt device performance to maximize energy generation in operational conditions while mitigating hydrodynamic loads in extreme waves to reduce the structural mass and overall cost. This paper formulates the optimal control problem to incorporate metrics that provide a measure of the surge restraining force, pitch restraining torque, and PTO control force. The optimizer must now handle an objective function with competing terms in an attempt to maximize power capture while minimizing structural and actuator loads. A penalty weight is placed on the surge restraining force, pitch restraining torque, and PTO actuation force, thereby allowing the control focus to be placed either on power absorption or load mitigation. Thus, in achieving these goals, a per-unit gain in TAP would not lead to a greater per-unit demand in structural strength, hence yielding a favorable benefit-to-cost ratio. Demonstrative results in the form of TAP, reactive TAP, and the amplitudes of the surge restraining force, pitch restraining torque, and PTO control force are shown for the Berkeley Wedge example.

INTRODUCTION

The Berkeley Wedge [1] is an asymmetric wave energy converter (WEC) and breakwater. It consists of an asymmetric floater, a power take-off (PTO) system, and a support structure. The particular shape of the floater, depicted in Fig. 1, was designed to experience minimal effects from viscosity in heave motion. The mounting structure limits the motion of the floater to heave only. The PTO system implemented in the design is a linear permanent magnet generator (LPMG) [2] . When the damping of the LPMG is matched with the heave radiation damping of the floater at resonance, there will be almost no radiated or transmitted waves and almost all of the incident wave energy will be absorbed by the damping of the LPMG. The Berkeley Wedge can be used near shore to provide electricity for local communities and act as a breakwater (concurrently) to protect the harbor with very minimal environmental impact. It can also be attached to offshore structures and floating platforms to provide electricity and protect the structure. In a recent study [3], the particular asymmetric shape of the Berkeley Wedge was implemented in a coaxial wave energy converter (consisting of a fixed inner cylinder and moving outer cylinder) to reduce the viscous effects

[*]Address all correspondence to this author.
[†]Ph.D candidate UC Berkeley, major field Ocean Engineering.
[‡]Director, Marine Mechanics Laboratory (MML), University of California at Berkeley.

on the heave motion of the outer cylinder. The straight-side of the inner cylinder mimics the backside of the two-dimensional Berkeley Wedge and its special shape has minimal viscous effects. The experimental testing revealed that the shape of the Berkeley Wedge reduced the viscous damping on the heave displacement of the outer cylinder by 70%, resulting in an increase in the heave displacement of the outer cylinder by more than 300%.

The success of such or similar future WEC technologies will require the development of control strategies that can adapt device performance to maximize energy generation in operational conditions while mitigating hydrodynamic loads in extreme waves to reduce the structural mass and overall cost [4]. Balancing these objectives offers an interesting design and control challenge. For example, they are in contrast to previous works that solved the optimal control problem when focused solely on maximizing the time-averaged power (TAP). The application of state-constrained optimization [5, 6] to WEC control has gained significant traction recently as it provides the ability to include linear and nonlinear constraints. This optimization has been pursued using calculus of variations [5], model predictive control [7–9], and pseudo-spectral methods [10–12]. If the PTO and structural loads are not considered, the optimum WEC trajectory follows that of complex conjugate control [13], which is known to require a substantial amount of reactive power when moving away from the resonance frequency. Suboptimal strategies that eliminate reactive power, notably latching [14] and declutching [15], have been proposed, yet still do not include a load metric in the optimization. It can be expected that as the controller works to maximize the absorbed mechanical energy, the growth rate in structural loads may exceed the growth in TAP. To address this concern, this work incorporates the restraining loads in the objective function of the optimization routine. As a result, the optimizer must now balance the opposing contributions in an attempt to obtain the largest power-to-load ratio.

This paper begins by describing the Berkeley Wedge device concept. This is followed by construction of the heave time-domain equation of motion to provide the preliminaries for extension into its spectral representation. The upper and lower bounds on the TAP, surge-restraining force, pitch-restraining torque, and PTO actuator force are calculated while assuming that the WEC motion was constrained but remains sinusoidal. The upper bound was calculated assuming an optimum phase between the heave wave-exciting force and heave velocity while the lower bound assumes that the PTO system consists only of a linear resistive damper, and in both cases the PTO force coefficients are constant and continuous throughout the wave cycle. Next, pseudo-spectral control theory is reviewed followed by incorporating the surge-restraining force, pitch-restraining torque, and PTO actuator force into the optimization problem. A penalty weight is placed on the contributions to the objective function from the restraining and PTO loads to allow the desired performance to be achieved. The effect of including the restraining loads on balancing power absorption and load shedding is first explored by varying the penalty weight magnitudes and comparing against the known performance bounds. The time history of WEC motion and PTO control force are presented to illustrate how per-unit increases in TAP can exceed the per-unit increase in restraining and PTO loads while having a minimal reactive power requirement.

Table 1. GEOMETRIC VALUES OF THE BERKELEY WEDGE.

Water Depth, h, 1.5 m	Draft, d, 0.7 m
Beam, b, 0.212 m	Area, S, 0.0677 m^2
Center of Gravity, x_g, -0.0848 m	Resonance, T_{res}, 1.25 s

THE BERKELEY WEDGE

The Berkeley Wedge shape was designed to experience the smallest effect from viscosity when encountering incident waves and in motion. The motion of the floater (shown in Fig. 1) is restricted to heave only. The physical dimensions of the asymmetric floater were chosen to fit the model testing facility at the University of California at Berkeley. A detailed theoretical and experimental study [1] confirmed the effectiveness of the design in reducing the viscous effect on the motion of the device, thereby capturing almost all of the incident wave energy and providing a calm water surface leeward of the asymmetric floater.

In this study, the authors examined the Berkeley Wedge with the physical dimensions given in Table 1. The particular shape of the floater (Fig. 1) can be obtained from:

$$\mathscr{F}(\bar{y}) = 0.05926(\bar{y}+1)^2 + 3.88147(\bar{y}+1)^3 - 2.94074(\bar{y}+1)^4 \quad (1)$$

In Eqn. (1), $\bar{x} = \mathscr{F}(\bar{y})$ is a shaping function, and $\bar{x} = x/b$ and $\bar{y} = y/d$ are nondimensional scales. In this equation, $\bar{y}$ can be shifted to obtain different drafts. The hydrodynamics coefficients for the asymmetric floater were obtained from the two-dimensional (2D) potential-flow code RWYADMXA [16] and shown in nondimensional form in Fig. 2. The resonance frequency, as reported in Table 1, is the frequency of maximum motion in regular-wave excitation. The natural frequency is the frequency of oscillation with an initial displacement or impulsive velocity. The two are close but not identical, primarily because the hydrodynamic coefficients are frequency dependent [17].

TIME-DOMAIN-HEAVE EQUATION OF MOTION

The one-degree-of-freedom time-domain-heave equation of motion is given by:

$$m\ddot{\zeta}_2(t) = f_{e2}(t) + f_{r22}(t) + f_h(t) + f_d(t) + f_m(t) \quad (2)$$

where t is time, m is the mass of the WEC, $\ddot{\zeta}_2$ is the heave acceleration, f_{e2} is the wave-exciting heave force caused by the incident

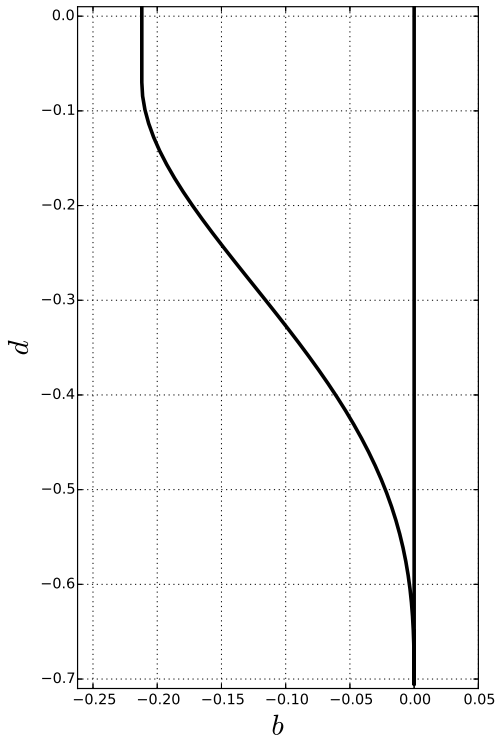

Figure 1. 2D SHAPE OF THE BERKELEY WEDGE WITH THE BEAM $(b) = 0.212\ m$ AND DRAFT $(d) = 0.7\ m$.

waves, f_{r22} is the wave radiation force caused by heave motion, f_h is the hydrostatic restoring force, f_d is the drag force caused by viscous effects, and f_m is the mechanical force applied by the PTO system.

The heave hydrostatic restoring force is given by:

$$f_h(t) = -C_{22}\zeta_2(t), \quad \text{with} \quad C_{22} = \rho g b \tag{3}$$

where ρ is the fluid density, g is the gravitational acceleration, b is the device beam length at the calm water line, and ζ_2 is the time-varying heave displacement.

The linear hydrodynamic wave-radiation heave force will be represented in the time domain using the Cummins equation [18] and is written as follows:

$$f_{r22}(t) = -\mu_{22}(\infty)\ddot{\zeta}_2(t) - \int_{-\infty}^{t} K_{r22}(t-\tau)\dot{\zeta}_2(\tau)\,d\tau \tag{4}$$

where $\mu_{22}(\infty)$ is the heave-added mass at infinite frequency, and K_{r22} is the heave radiation impulse response function, also known as the memory function because it represents the wave

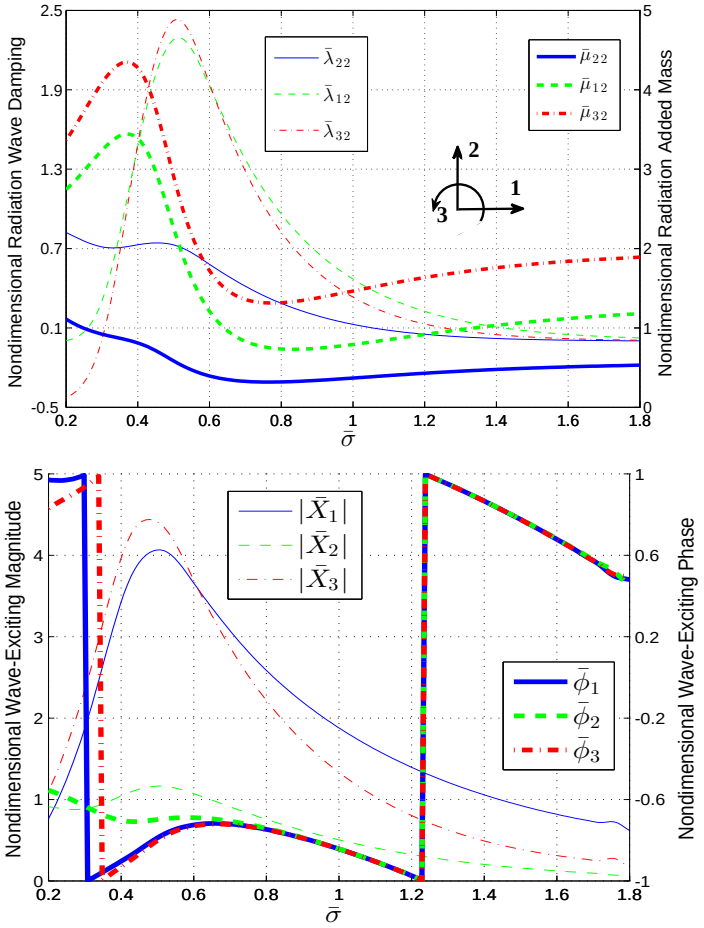

Figure 2. NONDIMENSIONAL 2D HYDRODYNAMIC RADIATION AND WAVE-EXCITING COEFFICIENTS[1].

radiation memory effect caused by past WEC motions. The relations between the time- and frequency-domain radiation coefficients were derived in [19]:

$$K_{r22}(t) = \frac{2}{\pi}\int_0^{\infty} \lambda_{22}(\sigma)\cos(\sigma t)\,d\sigma \tag{5}$$

$$K_{r22}(t) = -\frac{2}{\pi}\int_0^{\infty} \sigma\left[\mu_{22}(\sigma) - \mu_{22}(\infty)\right]\sin(\sigma t)\,d\sigma \tag{6}$$

where $\mu_{22}(\sigma)$ and $\lambda_{22}(\sigma)$ are the frequency-dependent hydrodynamic radiation coefficients commonly known as the added mass and wave radiation damping.

The wave-exciting heave force can be written in the time domain as follows:

$$f_{e2}(t) = \int_{-\infty}^{\infty} K_{e2}(t-\tau)\eta(\tau)\,d\tau \tag{7}$$

[1] $\bar{\sigma} = \sigma\sqrt{b/g}$, $\bar{\mu}_{22} = \mu_{22}/\rho b^2$, $\bar{\lambda}_{22} = \lambda_{22}/\rho b^2\sigma$, $\bar{X}_2 = X_2/\rho g b$, $\bar{\phi}_2 = \phi_2/\pi$, $\bar{\mu}_{12} = \mu_{12}/\rho b^2$, $\bar{\lambda}_{12} = \lambda_{12}/\rho b^2$, $\bar{X}_1 = X_1/\rho g b$, $\bar{\phi}_1 = \phi_1/\pi$, $\bar{\mu}_{32} = \mu_{32}/\rho b^3$, $\bar{\lambda}_{32} = \lambda_{32}/\rho b^3\sigma$, $\bar{X}_3 = X_3/\rho g b^2$, $\bar{\phi}_3 = \phi_3/\pi$

where K_{e2} is the heave wave-excitation kernel, which is non-causal, and η is the wave elevation. The relationship between the time- and frequency-domain excitation coefficients is given by:

$$K_{e2}(t) = \frac{1}{\pi}\int_0^\infty \left[\Re\left\{X_2(\sigma)\right\}\cos(\sigma t) - \Im\left\{X_2(\sigma)\right\}\sin(\sigma t)\right] d\sigma \quad (8)$$

where X_2 is the frequency-dependent complex wave-exciting heave-force coefficient, $\Re$ is the real component, and $\Im$ is the imaginary component.

The drag force is represented by either of the following:

$$f_d(t) = \begin{cases} -\lambda_{vl}\dot{\zeta}_2(t) \\ -\lambda_{vn}\dot{\zeta}_2(t)\left|\dot{\zeta}_2(t)\right| \end{cases} \quad (9)$$

where λ_{vl} is the linear-drag coefficient caused by the presence of viscosity, and λ_{vn} is the quadratic-drag coefficient, assuming they are not negligible. The final one-degree-of-freedom heave equation of motion can now be written as:

$$\begin{aligned}(m+\mu_{22}(\infty))\,\ddot{\zeta}_2(t) = &-C_{22}\zeta_2(t) - \lambda_{vl}\dot{\zeta}_2(t) \\ &- \int_{-\infty}^{t} K_{r22}(t-\tau)\,\dot{\zeta}_2(\tau)\,d\tau \\ &+ \int_{-\infty}^{\infty} K_{e2}(t-\tau)\,\eta(\tau)\,d\tau + f_m(t)\end{aligned} \quad (10)$$

where the linear form of the drag force has been used.

Regular Wave Analysis

It is common practice to begin analysis under regular wave excitation in which the incident wave elevation is described by:

$$\eta(x,t) = \Re\left\{-\frac{1}{g}\frac{\partial\phi_I}{\partial t}\bigg|_{z=h}\right\} = \Re\left\{Ae^{i(\sigma t - kx)}\right\} = A\cos(\sigma t - kx) \quad (11)$$

where η is the wave elevation, ϕ_I is the incident wave potential, A is the wave amplitude, σ is the wave angular frequency, k is the wave number, and $i = \sqrt{-1}$ is the imaginary unit. The time-harmonic heave response is then given by:

$$\zeta_2(t) = \Re\left\{\xi_2 e^{i\sigma t}\right\} \quad (12)$$

where ξ_2 is the complex amplitude of heave displacement.

Under regular wave excitation, the radiation-convolution integral can be simplified to:

$$f_{r22}(t) = -\Re\left\{\left[-\sigma^2\mu_{22}(\sigma) + i\sigma\lambda_{22}\right]\xi_2 e^{i\sigma t}\right\} \quad (13)$$

The wave-excitation-convolution integral can be written as:

$$f_{e2}(t) = \Re\left\{AX_2(\sigma)\,e^{i\sigma t}\right\} \quad (14)$$

For the time being, the mechanical force from the PTO system will be described by the following:

$$f_m(t) = -\Re\left\{\left(C_g - \sigma^2\mu_g + i\sigma B_g\right)\xi_2 e^{i\sigma t}\right\} \quad (15)$$

where C_g is the linear PTO-restoring coefficient, B_g is the PTO linear-damping coefficient, and μ_g is the additional PTO inertia. The frequency-domain expressions can be inserted into Eqn. (10), leading to the heave-displacement response amplitude operator:

$$\frac{\xi_2}{A} = \frac{X_2}{\left[C_{22} - \sigma^2(m+\mu_{22}) + C_g - \sigma^2\mu_g\right] + i\sigma\left[\lambda_{22} + B_g\right]} \quad (16)$$

where λ_{vl} has been set to zero since results as [1] saw minimal effects from viscosity.

PTO Absorbed Power The TAP absorbed by the PTO is calculated from:

$$\frac{P_T}{A^2} = \frac{1}{2}B_g\sigma^2\left|\frac{\xi_2}{A}\right|^2 \quad (17)$$

Equation (16) can be inserted into Eqn. (17) to calculate the optimal PTO damping at each wave frequency. The optimal, unconstrained, time-averaged absorbed power and PTO damping for each wave frequency is given by:

$$\left.\frac{P_T}{A^2}\right|_p = \frac{1}{4}\frac{|X_2|^2}{\lambda_{22}}\frac{1}{1+\sqrt{1+\left(\frac{C_{22}+C_g-\sigma^2(m+\mu_{22}+\mu_g)}{\sigma\lambda_{22}}\right)^2}} \quad (18)$$

$$B_g|_p = \lambda_{22}\sqrt{1+\left(\frac{C_{22}+C_g-\sigma^2(m+\mu_{22}+\mu_g)}{\sigma\lambda_{22}}\right)^2} \quad (19)$$

where at resonance $B_g = \lambda_{22}$, leading to the maximum time-averaged absorbed power [20]. Because these expressions do not consider motion constraints, it may be necessary to increase the PTO damping to remain under a given limit. The required PTO damping is given by:

$$\begin{aligned}B_g|_{pc} = &\left\{\left(\frac{A|X_2|}{\sigma|\xi_2|_{max}}\right)^2\right. \\ &\left.-\left[\frac{C_{22}+C_g}{\sigma} - \sigma(m+\mu_{22}+\mu_g)\right]^2\right\}^{1/2} - \lambda_{22}\end{aligned} \quad (20)$$

where $|\xi_2|_{max}$ is the maximum amplitude of heave displacement [21].

To provide a measure of efficiency for a given device, the TAP contained within a propagating wave must be known. The time-averaged wave power per-unit width, P_w, can be obtained from:

$$P_w = \frac{1}{2}\rho g A^2 V_g = \frac{1}{4}\rho g A^2 \sqrt{\frac{g}{k}\tanh kh}\left[1+\frac{2kh}{\sinh 2kh}\right] \quad (21)$$

where V_g is the wave group velocity, and h is the water depth.

Maximum Power Under Constrained Motion The maximum power absorption under motion constraints, while assuming sinusoidal motion, was explored in [22], which led to the following expression:

$$\left.\frac{P_T}{A^2}\right|_{mc} = \frac{1}{8}\frac{|X_2|^2}{\lambda_{22}}\left[1-H(1-\delta)(1-\delta)^2\right] \quad (22)$$

where $H(x)$ is the Heaviside step function, and δ is the ratio between the constrained-to-optimal heave velocity given by:

$$\delta = \frac{\sigma|\xi_2|_{max}}{A}\frac{2\lambda_{22}}{|X_2|} \quad (23)$$

Equation (22) can be expanded to show the trends in time-averaged absorbed power for the ranges of δ:

$$P_T|_{mc} = \begin{cases} \frac{1}{8}A^2|X_2|^2/\lambda_{22} & \delta > 1 \\ \frac{1}{2}A|X_2|\sigma|\xi_2|_{max} - \lambda_{22}\sigma^2|\xi_2|^2_{max} & \delta < 1 \end{cases} \quad (24)$$

The capture width, defined as the ratio between the TAP absorbed by the PTO and the incident wave power per-unit width, is a metric used to evaluate the absorption efficiency of the device. The incident wave power is proportional to the incident wave amplitude squared, see Eqn. (21). For unconstrained motion, which may also correspond to a very small incident wave amplitude, the capture width will be invariant to the incident wave height; whereas for a strongly constrained motion, which may also correspond to a very large incident wave amplitude, the capture width will be inversely proportional to the incident wave height and become less efficient.

The associated PTO linear-damping coefficient to observe the motion constraint is given by:

$$B_g|_{mc} = \lambda_{22}\left[1+\frac{2(1-\delta)}{\delta}H(1-\delta)\right] = \begin{cases} \lambda_{22} & \delta > 1 \\ \frac{A|X_2|}{\sigma|\xi_2|_{max}} - \lambda_{22} & \delta < 1 \end{cases} \quad (25)$$

where the PTO spring and inertia coefficients cancel the dynamic force contribution from the natural body-restoring coefficient, mass, and hydrodynamic added mass:

$$C_g - \sigma^2\mu_g = -\left[C_{22} - \sigma^2(m+\mu_{22})\right] \quad (26)$$

which is the basis of complex conjugate control [13]. Often in power quality management it is desirable to have the peak-to-average power ratio as close as possible to eliminate the need for advanced signal conditioning. Under complex conjugate control the peak-to-average power ratio, $P_\pm$, is given by [21, 23]:

$$P_\pm = 1 \pm \sqrt{1+\left[\frac{C_{22}-\sigma^2(m+\mu_{22})}{\sigma B_g}\right]^2} \quad (27)$$

When there is no reactive power, $X_g = \sigma\mu_g - C_g/\sigma = 0$, the peak-to-average power ratio is 2 and the instantaneous power oscillates between 0 and $2P_T$. The reactive component is eliminated at the resonance frequency of the isolated floating body and the peak-to-average power ratio is minimized at 2; however, when away from the resonant frequency, the peak-to-average power ratio quickly increases, resulting in large swings in the bidirectional energy flow.

Foundation Reaction Force and Moment

The structural foundation must handle the reaction force and torque needed to restrain the WEC to heave motion. The reaction force and torque in surge, X_{r1}, and pitch, X_{r3}, are given by:

$$A(X_{r1}+X_1) = \left[-\sigma^2\mu_{12} + i\sigma\lambda_{12}\right]\xi_2 \quad (28)$$

$$A(X_{r3}+X_3) = \left[-\sigma^2(x_g m+\mu_{32}) + i\sigma\lambda_{32}\right]\xi_2 \quad (29)$$

where X_1 and X_3 are the complex surge wave-exciting force and pitch wave-exciting torque coefficients per unit wave amplitude, μ_{12} is the surge-heave added mass, and λ_{12} is the surge-heave wave radiation damping, μ_{32} is the pitch-heave added mass, λ_{32} is the pitch-heave wave radiation damping, and x_g is the horizontal center of gravity. The surge and pitch foundation reaction force and torque are affected by the heave motion of the WEC, which can be controlled by the PTO. The time-domain corollary of Eqns. (28) and (29) is given by:

$$f_{r1}(t) = -\int_{-\infty}^{\infty} K_{e1}(t-\tau)\eta(\tau)\,d\tau + \mu_{12}(\infty)\ddot{\zeta}_2(t) + \int_{-\infty}^{t} K_{r12}(t-\tau)\dot{\zeta}_2(\tau)\,d\tau \quad (30)$$

$$f_{r3}(t) = -\int_{-\infty}^{\infty} K_{e3}(t-\tau)\eta(\tau)\,d\tau + (x_g m+\mu_{32}(\infty))\ddot{\zeta}_2(t) + \int_{-\infty}^{t} K_{r32}(t-\tau)\dot{\zeta}_2(\tau)\,d\tau \quad (31)$$

Results from Fixed-PTO Coefficients

Maximizing the TAP, as described in previous sections, involves the PTO coefficients to be fixed in time although adapted for a given wave amplitude and angular frequency. Performance bounds can be set for the TAP, surge-restraining force amplitude, pitch-restraining torque amplitude, and PTO control force amplitude, which have been plotted in Fig. 3. A benefit of the current design can be observed in the bottom plot of Fig. 3, where the heave amplitude and phase required for elimination of the surge-restraining force and pitch-restraining torque are presented. The surge and pitch components require a very similar amplitude and phase for elimination, which will lead to a reduction in both if only one contribution is heavily penalized in the controller. It is expected that time-varying PTO coefficients can help optimize the time-averaged absorbed power while reducing loads, leading to device performance that sits between the maximum constrained and passive curves.

PSEUDO-SPECTRAL CONTROL

The discretization of the control problem is completed by approximating the heave velocity and PTO force with a linear combination of basis functions [11, 24]. The heave velocity, ζ_2, and PTO force, f_m, are approximated by a zero-mean truncated Fourier series with N terms:

$$\dot{\zeta}_2(t) \approx \sum_{j=1}^{N/2} \psi_j^c \cos(j\sigma_0 t) + \psi_j^s \sin(j\sigma_0 t) = \Phi(t)\hat{\psi} \quad (32)$$

$$f_m(t) \approx \sum_{j=1}^{N/2} \tau_j^c \cos(j\sigma_0 t) + \tau_j^s \sin(j\sigma_0 t) = \Phi(t)\hat{\tau} \quad (33)$$

where

$$\hat{\psi} = \left[\psi_1^c, \psi_1^s, \ldots, \psi_{\frac{N}{2}}^c, \psi_{\frac{N}{2}}^s\right]^\top, \ \hat{\tau} = \left[\tau_1^c, \tau_1^s, \ldots, \tau_{\frac{N}{2}}^c, \tau_{\frac{N}{2}}^s\right]^\top \quad (34)$$

$$\Phi(t) = [\phi_1(t), \phi_2(t), \ldots, \phi_{N-1}(t), \phi_N(t)] \quad (35)$$

$$= \left[\cos(\sigma_0 t), \sin(\sigma_0 t), \ldots, \cos\left(\frac{N}{2}\sigma_0 t\right), \sin\left(\frac{N}{2}\sigma_0 t\right)\right]$$

with the fundamental frequency given by $\sigma_0 = 2\pi/T$ and T is the chosen time duration. The heave equation of motion can be described as follows:

$$M_{22}\hat{\psi} = \hat{\tau} + \hat{e}_2 \quad (36)$$

where $\hat{e}_2$ is the Fourier coefficient vector of the heave wave-exciting force. The matrix $M_{22} \in \mathbb{R}^{N\times N}$ is block diagonal with the following structure:

$$M_{22}^j = \begin{bmatrix} \lambda_{22}(j\sigma_0) & \alpha(j\sigma_0) \\ -\alpha(j\sigma_0) & \lambda_{22}(j\sigma_0) \end{bmatrix} \quad \text{for} \quad j = 1, 2, \ldots, N/2$$

$$\alpha(j\sigma_0) = j\sigma_0(m + \mu_{22}(j\sigma_0)) - C_{22}/(j\sigma_0) \quad (37)$$

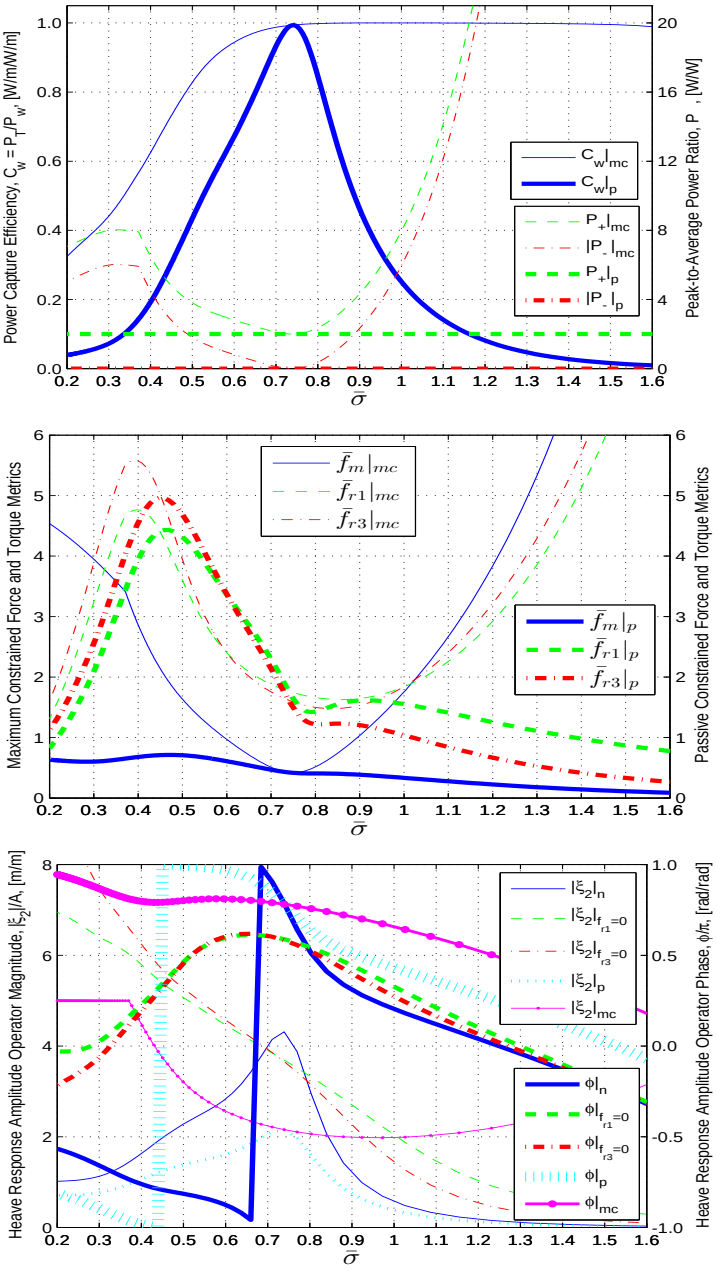

Figure 3. PERFORMANCE BOUNDS UNDER A HEAVE-DISPLACEMENT AMPLITUDE CONSTRAINT OF 0.1 M AND A WAVE AMPLITUDE OF 0.02 M. THE SUBSCRIPT $_p$ DENOTES PASSIVE PERFORMANCE AS GIVEN BY EQNS. (17)–(20). THE SUBSCRIPT $_{mc}$ DENOTES MAXIMUM CONSTRAINED PERFORMANCE AS GIVEN BY EQNS. (22)–(26). THE SUBSCRIPT $_n$ DENOTES THE NATURAL HEAVE MOTION (NO PTO), WHEREAS $f_{r1} = 0$ AND $f_{r3} = 0$ DENOTE HEAVE MOTION REQUIRED TO ELIMINATE THE SURGE-RESTRAINING FORCE AND PITCH-RESTRAINING TORQUE. THE NONDIMENSIONAL FORCE AND TORQUE VALUES ARE GIVEN BY: $\bar{f}_m = f_m/\rho g b A$, $\bar{f}_{r1} = f_{r1}/\rho g b A$, AND $\bar{f}_{r3} = f_{r3}/\rho g b^2 A$.

The heave velocity coefficients can then be determined explicitly from the control and heave wave-exciting force Fourier coefficients. This representation allows the total absorbed energy, E, to be written as:

$$E = -\int_0^T \dot{\zeta}_2(t) f_m(t)\, dt = -\frac{T}{2}\hat{\psi}^\top \hat{\tau} = -\frac{T}{2}\left[\hat{\tau}^\top \left(M_{22}^{-1}\right)^\top \hat{\tau} + \hat{e}_2^\top \left(M_{22}^{-1}\right)^\top \hat{\tau}\right] \quad (38)$$

which is in the form of a traditional quadratic problem.

Penalty Terms

Surge Foundation Force Load reduction will consist of limiting the forces on the WEC structure that are required to maintain the heave-only constraint. This force has two contributions that arise from the surge wave-exciting force and WEC motion. The equation for the surge foundation force can be written in a matrix form, similar to Eqn. (36), as follows:

$$\begin{aligned}\Phi(t)\hat{f}_{r1} &= -\Phi(t)\hat{e}_1 + \mu_{12}(\infty)\Gamma\hat{\psi} + \Phi(t)\left(G_{12} - \mu_{12}(\infty)\Gamma\right)\hat{\psi} \\ \hat{f}_{r1} &= -\hat{e}_1 + G_{12}\hat{\psi} = -\hat{e}_1 + G_{12}M_{22}^{-1}\hat{\tau} + G_{12}M_{22}^{-1}\hat{e}_2 \end{aligned} \quad (39)$$

where $\hat{e}_1$ is the Fourier coefficients of the surge wave-exciting force, G_{12} and Γ are block matrices given in Appendix A and Eqn. (36) has been substituted in the last expression. To maintain the convexity of the quadratic problem, the squared ℓ^2-norm of the surge-foundation force vector was added to the objective function. The objective function is given by:

$$\begin{aligned}\gamma_1|f_{r1}|^2 &= \gamma_1 \int_0^T \hat{f}_{r1}^\top \Phi(t)^\top \Phi(t)\hat{f}_{r1}\, dt = \frac{T}{2}\hat{f}_{r1}^\top \hat{f}_{r1} \\ &\approx \gamma_1 \frac{T}{2}\left(2\left[\hat{e}_1^\top G_{12}M_{22}^{-1} - \hat{e}_2^\top \left(M_{22}^{-1}\right)^\top G_{12}^\top G_{12}M_{22}^{-1}\right]\hat{\tau} \right. \\ &\quad \left. -\hat{\tau}^\top \left(M_{22}^{-1}\right)^\top G_{12}^\top G_{12}M_{22}^{-1}\hat{\tau}\right) \end{aligned} \quad (40)$$

where γ_1 is a penalty weight applied to the surge foundation force. In the final expression for the surge-foundation force contribution, there are three constant terms independent of the PTO control force, which are left out of the optimization. See [12] for the full expression.

Pitch Foundation Torque Similar to the surge-restraining force, the pitch-restraining torque has two contributions that arise from the pitch wave-exciting torque and WEC motion. The matrix form of the pitch-restraining torque can be written as:

$$\hat{f}_{r3} = -\hat{e}_3 + G_{32}\hat{\psi} = -\hat{e}_3 + G_{32}M_{22}^{-1}\hat{\tau} + G_{32}M_{22}^{-1}\hat{e}_2 \quad (41)$$

where $\hat{e}_3$ represents the Fourier coefficients of the pitch wave-exciting torque. As with the surge-restraining force, the squared ℓ^2-norm of the pitch-restraining torque vector was added to the objective function. The pitch foundation torque measure is given by:

$$\begin{aligned}\gamma_3|f_{r3}|^2 &= \gamma_3 \int_0^T \hat{f}_{r3}^\top \Phi(t)^\top \Phi(t)\hat{f}_{r3}\, dt = \frac{T}{2}\hat{f}_{r3}^\top \hat{f}_{r3} \\ &\approx \gamma_3 \frac{T}{2}\left(2\left[\hat{e}_3^\top G_{32}M_{22}^{-1} - \hat{e}_2^\top \left(M_{22}^{-1}\right)^\top G_{32}^\top G_{32}M_{22}^{-1}\right]\hat{\tau} \right. \\ &\quad \left. -\hat{\tau}^\top \left(M_{22}^{-1}\right)^\top G_{32}^\top G_{32}M_{22}^{-1}\hat{\tau}\right) \end{aligned} \quad (42)$$

where γ_3 is a penalty weight applied to the pitch foundation torque.

PTO Control Force Magnitude The PTO force is the only control actuation, and in an effort to reduce computational time and force spikes, a penalty weight was placed on the squared ℓ^2-norm of the PTO force magnitude [7]:

$$\beta_m|\tau_m|^2 = \int_0^T \beta_m \tau_m(t)\tau_m(t)dt = \frac{T}{2}\hat{\tau}^\top \beta_m I_N \hat{\tau} \quad (43)$$

where β_m is a penalty weight associated with the control force magnitude, and I_N is the identity matrix of size N.

Final Objective Function The objective function will be the sum of the time-averaged absorbed power, the squared ℓ^2-norm of the surge-restraining force, pitch-restraining torque, and control force magnitude. The four contributions to the objective function are not of the same units, and the interrelationship between them is complex. Therefore, the final objective function will consist of the following nondimensional quantities:

$$J = \frac{E}{P_w T} + \gamma_1\left|\frac{f_{r1}}{\rho g b A}\right|^2 + \beta_m\left|\frac{f_m}{\rho g b A}\right|^2 + \gamma_3\left|\frac{f_{r3}}{\rho g b^2 A}\right|^2 \quad (44)$$

PSEUDO-SPECTRAL RESULTS

As a result of the physical restrictions of the model-testing facility at the University of California at Berkeley [1], only model-scale waves were used for analysis; however, Froude scaling can be used to estimate device performance at the prototype level. The work presented in the paper was focused on confirmation of the controller concept and validation of the analysis.

Effect of Penalty Terms

Figure 4 verifies that the pseudo-spectral controller is achieving the desired results when considering the extremes of the tested penalty weights. As the control force penalty weight, β_m, is increased the magnitude of the PTO control force and reactive power is reduced. As shown for the lowest values of γ_1 and β_m, the highest TAP is achieved; however, a larger reactive power component is required. Whereas for the largest values of γ_1 and β_m, reduction in the surge-restraining force and pitch-restraining torque is counterbalanced by an increase in the PTO control force. The increase in PTO force is a result of

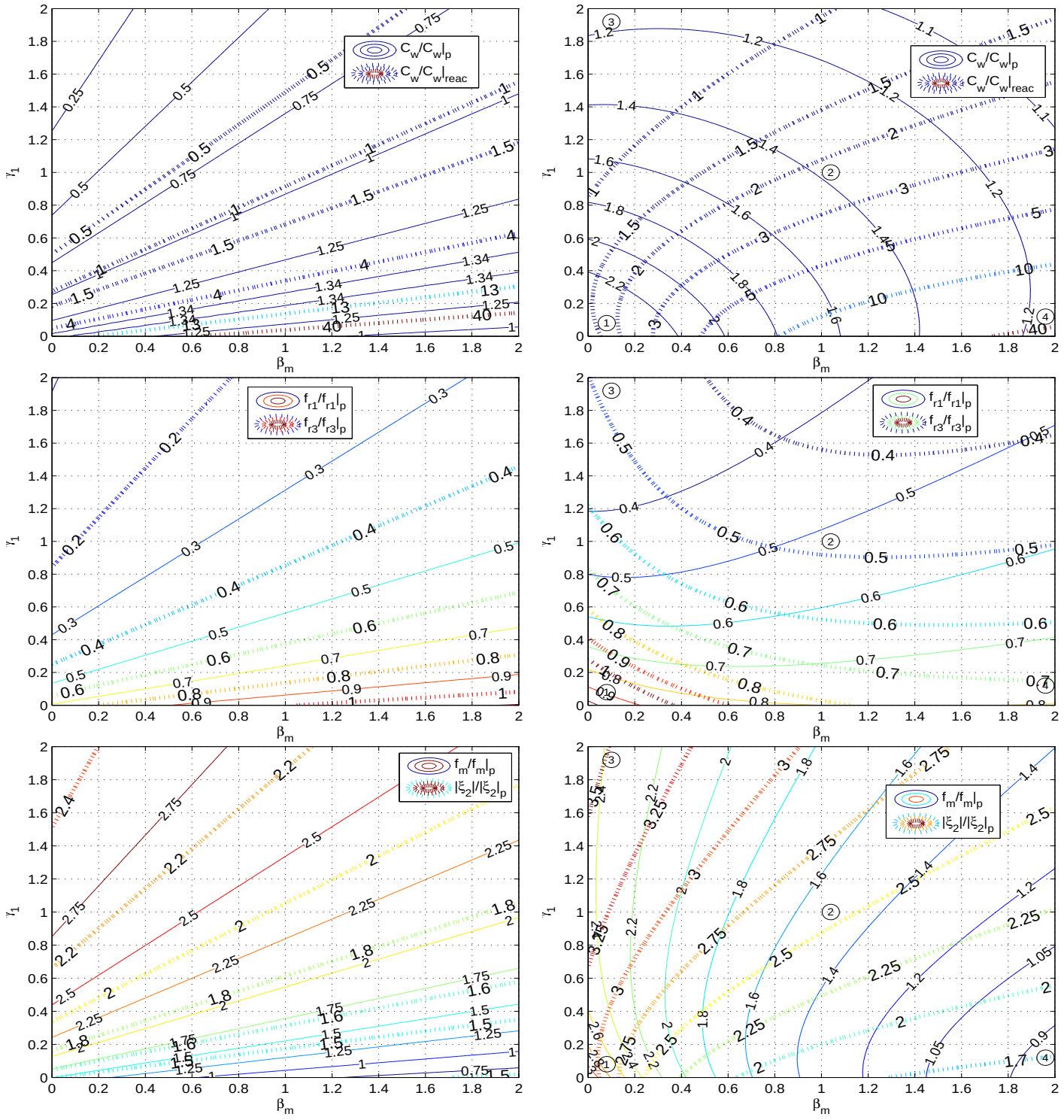

Figure 4. SENSITIVITY OF PERFORMANCE METRICS TO PENALTY WEIGHTS UNDER A HEAVE-DISPLACEMENT AMPLITUDE CONSTRAINT OF 0.1 M AND WAVE AMPLITUDE OF 0.02 M. THE LEFT COLUMN PLOTS RESULTS FOR A WAVE PERIOD OF 1.5 S ($\bar{\sigma} = 0.62$) AND THE RIGHT COLUMN FOR A WAVE PERIOD OF 1 S ($\bar{\sigma} = 0.92$). THE SUBSCRIPT $_p$ DENOTES PASSIVE PERFORMANCE AS GIVEN BY EQNS. (17)–(20).

the amplitude and phase difference between the unforced (no PTO) and zero surge-restraining force heave motion (refer to the bottom plot of Fig. 3). It can be observed that both above and below the resonance frequency the unforced heave amplitude of motion is lower than what is required for elimination of the surge-restraining force. As more emphasis is placed on reducing the surge-restraining force, greater control forces and reactive power are required, which implies that complete elimination of the restraining loads may not be desirable.

In Fig. 4, the region bounded by $\beta_m \geq 0.8$ and $\gamma_1 \leq 0.4$ is the most favorable as the capture efficiency can be increased between 20%–80% with a reactive power contribution comprising only 1/10th of the TAP. Furthermore, the surge-restraining force (f_{r1}), pitch-restraining torque (f_{r3}), and PTO control force can be reduced between 10%–30% with respect to the passive values; however, it is evident that the contours will vary depending on the incident wave frequency and most likely on the heave amplitude constraint. The left column of Fig. 4 plots a set of results for a wave frequency below resonance. In this frequency range the contours follow nearly straight lines when viewing the γ_1 and β_m space. Here the greatest difference in the heave motion amplitude and phase occurs, requiring a proportionate increase in the PTO control force to decrease restraining loads. Just below resonance the TAP curve decreases slower than above resonance; however, a greater control effort will be needed to reduce restraining loads. These contour plots provide a clear design space that can be used to optimize power production, decrease structural loads, or achieve many combinations in between.

Time History of WEC and PTO

Figure 5 plots the time history of the four points marked in the plots along the right column of Fig. 4. In region 1 the maximum power absorption is nearly recovered, in region 2 there is roughly a 50% reduction for all performance metrics compared to maximum absorption, in region 3 the surge-restraining force is prioritized at the expense of larger PTO forces and reactive power, and in region 4 the controller attempts to maximize TAP with reduced PTO forces at the expense of larger restraint loads. As the penalty weights are reduced, the PTO control force moves the heave velocity closer in phase with the heave wave-exciting force. This phase shift is accompanied by the greatest amplitudes in PTO control force, surge-restraining force and pitch-restraining torque, but not reactive power. Marker 3 has the greatest reactive power requirement as the amplitude of motion to eliminate the surge-restraining force is greater than the maximum constrained heave profile. As the surge-restraint and PTO force penalty weights are increased, the controller will first maintain a near optimum phase while reducing the amplitude of motion; however, eventually a greater phase shift is introduced by the controller to eliminate a greater proportion of the surge-foundation force; refer to Eqn. (28). Further reduction in the restraint loads will then see an increase in the heave amplitude of motion and a corresponding increase in PTO control force and reactive power. The larger reduction in restraint loads and PTO force can be achieved because of the ability of the controller to induce a phase shift in the heave velocity at the expense of bidirectional energy flow, which can be greatly affected by PTO efficiency [25].

CONCLUSIONS

In this paper, we describe how pseudo-spectral optimal control was used to optimize the performance of a novel WEC/breakwater, the Berkeley Wedge. The analysis revealed that the power capture efficiency increases by 50% for lower frequencies ($\bar{\sigma} < 0.74$) compared to results obtained from a passive PTO with a constant linear damper. For frequencies greater than $\bar{\sigma} > 0.74$, a capture efficiency of unity can be achieved; however, as the wave frequency moves away from resonance a greater reactive power component is required. Though the maximum capture efficiency is lower below resonance, the surge-restraining force and pitch-restraining torque are also lower, in the range of $0.5 \leq \bar{\sigma} \leq 0.7$, for the maximum constrained heave motion than the passive. Thus, when operating slightly below the resonance frequency with a PTO that allows for bidirectional energy flow, lower restraint forces and torques will be observed, thereby leading to favorable power-to-load ratios. The magnitude and phase of heave motion required to cancel the surge-restraining force and pitch-restraining torque were calculated to show that greater PTO control forces and reactive power is required for achieving such performance.

The pseudo-spectral optimal control problem was improved by including the squared ℓ^2-norm of the surge-restraining force, pitch-restraining torque, and PTO actuator force in the objective function. The optimizer performance was found to be adjustable based on the values chosen for the separate penalty weights placed on the three load contributions; however, it was found that because of WEC dynamics reducing either the surge-restraint force or pitch-restraint torque would lead to a reduction in the other. Thus, penalizing one of the contributions in the objective function was sufficient to explore the power-to-load ratios. Two incident wave periods above and below the resonance frequency, with a wave amplitude of 0.02 m and maximum allowable heave displacement of 0.1 m, were used to analyze the pseudo-spectral controller. When the penalty weights $\gamma_1 \to 0$ and $\beta_m \to 0$, maximum power capture was recovered with minimal reduction in system loads. The case of $\gamma_1 \to \infty$ and $\beta_m \to \infty$ would significantly reduce restraint loads; however, at the expense of greater PTO forces and reactive power requirements. If the penalty weights are kept with the range of $\beta_m \geq 0.8$ and $\gamma_m \leq 0.4$, an increase in capture efficiency of 20% to 80% is obtainable with the reactive power comprising no more than 1/10th of the TAP.

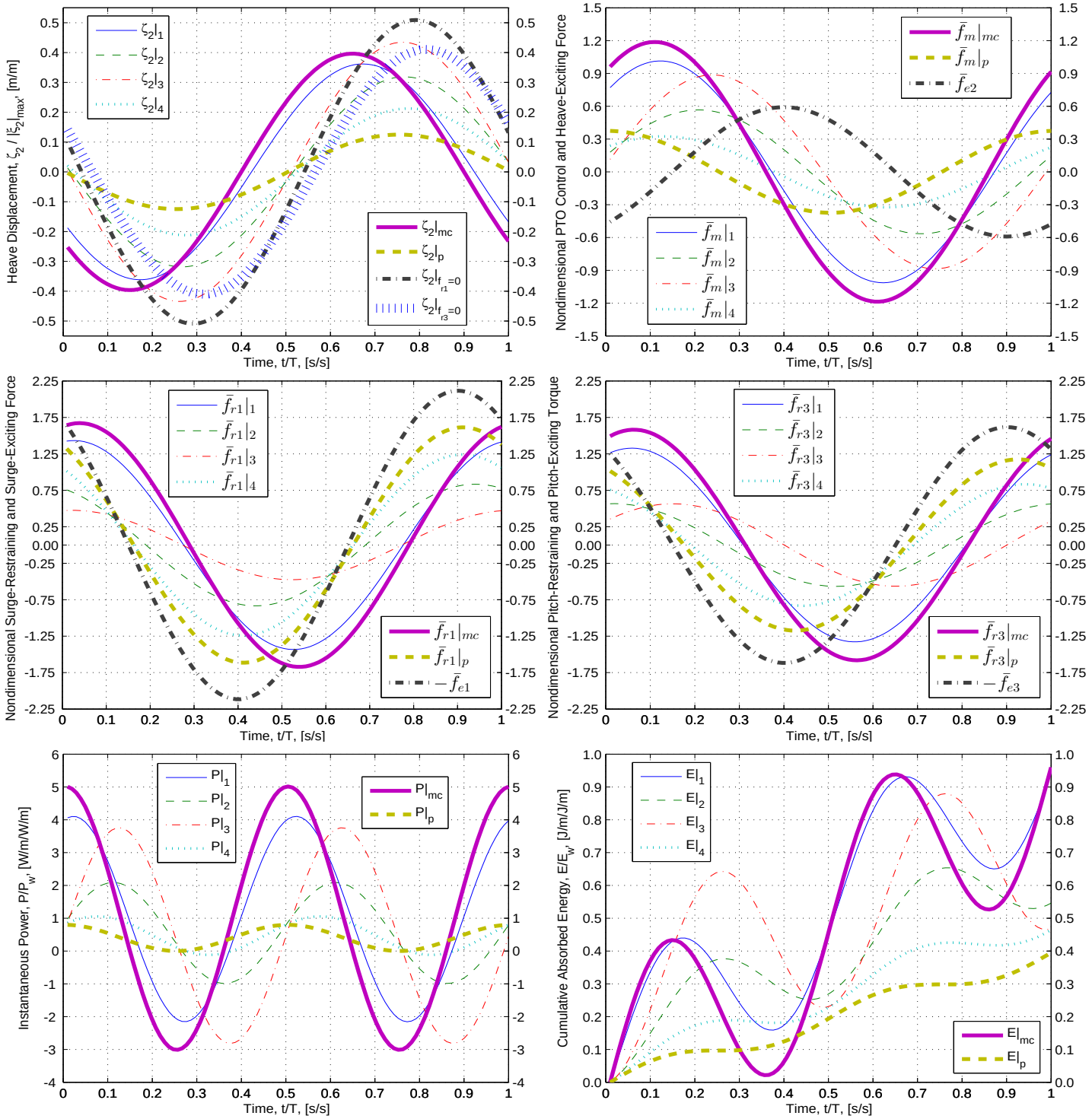

Figure 5. TIME HISTORY OF WEC MOTION, PTO CONTROL FORCE, PTO POWER, RESTRAINING FORCE, AND RESTRAINING TORQUE. RESULTS FROM APPLYING PSEUDO-SPECTRAL CONTROL WITH $T = 1$ s, $A = 2$ cm, AND VARYING PENALTY WEIGHTS. THE NUMBERS 1, 2, 3, AND 4 IN THE LEGEND REFER TO THE FOUR MARKERS IN THE TOP PLOT OF FIGURE 4. THE SUBSCRIPT $_p$ DENOTES PASSIVE PERFORMANCE AS GIVEN BY EQNS. (17)–(20). THE SUBSCRIPT $_{mc}$ DENOTES MAXIMUM CONSTRAINED PERFORMANCE AS GIVEN BY EQNS. (22)–(26). A HEAVE-DISPLACEMENT AMPLITUDE LIMIT OF 0.1 M WAS USED WHILE THE NUMBER OF FOURIER COEFFICIENTS WAS SET AT $N = 100$. E_w IS THE CUMULATIVE ABSORBED ENERGY WHEN ASSUMING PERFECT ABSORPTION.

In the same region, where the surge-restraining force and pitch-restraining torque were reduced between 20%–30% with little to no increase in PTO force. This work has highlighted some of the issues that arise when WEC control focuses solely on maximizing power absorption as it is accompanied by proportionately greater structural and PTO loads that lead to a higher levelized cost of energy. In the future, pursuit of moderate gains in TAP from control strategies may be more favorable as the increase in power absorption may outpace the growth in structural loads.

ACKNOWLEDGMENT

This work was supported by the U.S. Department of Energy under Contract No. DE-AC36-08GO28308 with the National Renewable Energy Laboratory. Funding for the work was provided by NREL's Laboratory Directed Research and Development (LDRD) Program.

REFERENCES

[1] Madhi, F., Sinclair, M. E., and Yeung, R. W., 2014, "The "Berkeley Wedge": an asymmetrical energy-capturing floating breakwater of high performance," Marine Systems & Ocean Technology, **9** (1), pp. 5-16.

[2] Tom, N. and Yeung, R. W., 2013, "Performance enhancements and validations of the UC-Berkeley ocean-wave energy extractor," ASME Journal of Offshore Mechanics Arctic Engineering, **134** (2), p. 041101.

[3] Son, D. H., Belissen, D., and Yeung, R. W., 2015, "Optimizing the Performance of a Dual Coaxial-Cylinder Wave-Energy Extractor," Proceedings of the ASME 2015 34th International Conference on Ocean, Offshore and Arctic Engineering (OMAE2015-42379), May 31-June 5, 2015, St. John's, Newfoundland, Canada.

[4] Musial, W., Lawson, M., Rooney, S., 2013, "Marine Hydrokinetic Technology (MHK) Instrumentation, Measurement, and Computer Modeling Workshop," NREL/TP-5000-57605, National Renewable Energy Laboratory, Boulder, CO.

[5] Eidsmoen, H., 1996, "Optimum control of a floating wave-energy converter with restricted amplitude," ASME Journal of Offshore Mechanics and Arctic Engineering, **118** (2), pp. 96–102.

[6] Hals, J., Falnes, J., Moan, T., 2011, "Constrained optimal control of a heaving buoy wave-energy converter," ASME Journal of Offshore Mechanics and Arctic Engineering, **133** (1), p. 011401.

[7] Cretel, J. A. M., Lightbody, G., Thomas, G. P., and Lewis, A. W., 2011, "Maximisation of energy capture by a wave-energy point absorber using model predictive control," Proceedings of the 18th World Congress of the International Federation of Automatic Control, Milano, Italy, 3714–3721.

[8] Abraham, E., Kerrigan, E. C., 2013, "Optimal active control and optimization of a wave energy converter," IEEE Transactions on Sustainable Energy, **4** (2), pp. 324–332.

[9] Li, G., Belmont, M. R., 2014, "Model predictive control of sea wave energy converters —Part I: A convex approach for the case of a single device," Renewable Energy, **69**, pp. 453-463.

[10] Bacelli, G. and Ringwood, J. V., 2011, "A Control System for a Self-reacting Point Absorber Wave Energy Converter Subject to Constraints," Proceedings of the 18th World Congress of the International Federation of Automatic Control, Milano, Italy, pp. 11387–11392.

[11] Herber, D. R., Allison, J. T., 2013, "Wave energy extraction maximization in irregular ocean waves using pseudospectral methods," Proceedings of the ASME International Design Engineering Technical Conferences and Computers and Information in Engineering Conference, Portland, OR, USA.

[12] Tom, N., Yu, Y. H., Lawson, M., and Wright, A. D., 2016, "Pseudo-spectral control of a novel oscillating surge wave energy converter in regular waves, part I: power optimization including load reduction," *Ocean Engineering*, (under review).

[13] Falnes, J., 2002, "Optimum control of oscillation of wave-energy converters," International Journal of Offshore and Polar Engineering, **12** (2), pp. 147–154.

[14] Babarit, A., and Clément, A. H., 2006, "Optimal latching control of a wave energy device in regular and irregular waves," Applied Ocean Research, **28**, pp. 77–91.

[15] Babarit, A., Guglielmi, M., and Clément, A. H., 2009, "Declutching control of a wave energy converter," Ocean Engineering, **36** (12), pp. 1015–1024.

[16] Yeung, R. W., 1975, "A hybrid integral-equation method for time-harmonic free surface flows," Proceedings of the 1st International Conference on Numerical Ship Hydrodynamics, Gaithersburg, MD, pp. 58–607.

[17] Yeung, R. W., 1982, "The transient heaving motion of floating cylinders," Journal of Engineering Mathematics, **16** (2), pp. 97–119.

[18] Cummins, W. E., 1962, "The impulse response function and ships motions. Schiffstechnik, **9**, pp. 101–109.

[19] Ogilvie, T., 1964, "Recent progress towards the understanding and prediction of ship motions," Proceedings of the Fifth Symposium on Naval Hydrodynamics, Bergen, Norway, Sept. 10-12, pp. 3–79.

[20] Evans, D. V., 1976, "A theory for wave-power absorption by oscillating bodies," Journal of Fluid Mechanics, **7** (1), pp. 1–25.

[21] Hals, J., Bjarte-Larsson, T., and Falnes, J., 2002, "Optimum reactive control and control by latching of a wave-absorbing semisubmerged heaving sphere," Proceedings of the 21st International Conference on Offshore Mechanics and Arctic Engineering, Oslo, Norway, June 22-28, pp. 415–423.

[22] Evans, D. V., 1981, "Maximum wave-power absorption under motion constraints," Applied Ocean Research, **3** (4), pp. 200–203.

[23] Tom, N., Yu, Y. H., Lawson, M., and Wright, A. D., 2016, "Pseudo-spectral control of a novel oscillating surge wave energy converter in regular waves, part II: nonlinear power optimization including load reduction," Ocean Engineering, (under review).

[24] Bacelli, G., and Ringwood, J. V., 2015, "Numerical Optimal Control of Wave Energy Converters," IEEE Transactions on Sustainable Energy, **6** (2), pp. 133–145.

[25] Genest, R., Félicien, B., Clément, A. H., and Babarit A., 2014, "Effect of non-ideal power take-off on the energy absorption of a reactively controlled one degree of freedom wave energy converter," Applied Ocean Research, **48**, pp. 236–243.

A Matrix Expressions

The time-derivative matrix, $\Gamma \in \mathbb{R}^{N\times N}$, is block diagonal with the following block structure:

$$\Gamma^j = \begin{bmatrix} 0 & j\sigma_0 \\ -j\sigma_0 & 0 \end{bmatrix} \quad \text{for} \quad j = 1,2,\ldots,N/2 \tag{45}$$

Using a change of variables, the surge-pitch radiation convolution integral can be represented in matrix form as follows:

$$\begin{aligned} f_{r12}(t) &= \int_{-\infty}^{t} K_{r12}(t-\tau)\,\dot{\zeta}_2(\tau)\,d\tau \\ &= \Phi(t)\,(G_{12} - \mu_{12}(\infty)\,\Gamma)\,\hat{\psi} \end{aligned} \tag{46}$$

where $G_{12} \in \mathbb{R}^{N\times N}$ is block diagonal with the following structure:

$$G_{12}^{j} = \begin{bmatrix} \lambda_{12}(j\sigma_0) & \sigma\mu_{12}(j\sigma_0) \\ -j\sigma_0\mu_{12}(j\sigma_0) & \lambda_{12}(j\sigma_0) \end{bmatrix} \text{ for } j = 1,2,\ldots,N/2 \quad (47)$$